A NOVEL ULTRASONIC METHOD FOR ACCURATE CHARACTERIZATION OF MICROSTRUCTURAL GRADIENTS IN MONOLITHIC AND COMPOSITE TUBULAR STRUCTURES

Don J. Roth, Dorothy V. Carney, George Y. Baaklini
National Aeronautics and Space Administration
Lewis Research Center
Cleveland, Ohio 44135

and

James R. Bodis, Richard W. Rauser
Cleveland State University
Cleveland, Ohio 44115

BACKGROUND

Prior studies have shown that ultrasonic velocity/time-of-flight imaging that uses back surface echo reflections to gauge volumetric material quality is well suited (perhaps more so than is the commonly-used peak amplitude c-scanning) for *quantitative* characterization of microstructural *gradients*. Such gradients include those due to pore fraction, density, fiber fraction, and chemical composition variations [11–15]. Variations in these microstructural factors can affect the uniformity of physical performance (including mechanical [stiffness, strength], thermal [conductivity], and electrical [conductivity, superconducting transition temperature], etc. performance) of monolithic and composite [1,3,6,12]. A weakness of conventional ultrasonic velocity/time-of-flight imaging (as well as to a lesser extent ultrasonic peak amplitude c-scanning where back surface echoes are gated [17] is that the image shows the effects of thickness as well as microstructural variations unless the part is uniformly thick. This limits this type of imaging's usefulness in practical applications. The effect of thickness is easily observed from the equation for pulse-echo waveform time-of-flight (2τ) between the first front surface echo (FS) and the first back surface echo (B1), or between two successive back surface echoes where:

$$2\tau = \frac{(2d)}{V} \tag{1}$$

where d is the sample thickness and V is the velocity of ultrasound in the material. Interpretation of the time-of-flight image is difficult as thickness variation effects can mask or overemphasize the true microstructural variation portrayed in the image of a part containing thickness variations. Thickness effects on time-of-flight can also be interpreted by rearranging equation (1) to calculate velocity:

$$V = \frac{2d}{2\tau} \tag{2}$$

such that velocity is inversely proportional to time-of-flight. Velocity and time-of-flight maps will be affected similarly (although inversely in terms of magnitude) by thickness variations, and velocity maps are used in this investigation to indicate time-of-flight variations.

SINGLE TRANSDUCER THICKNESS-INDEPENDENT ULTRASONIC VELOCITY MEASUREMENTS

Several [7,9,10,20] described a single point ultrasonic velocity measurement method using a reflector plate located behind and separated from the sample, that does not require prior knowledge of sample thickness. The latter, method was studied with success in prototypical scanning configurations for

Review of Progress in Quantitative Nondestructive Evaluation, Vol. 18
Edited by Thompson and Chimenti, Kluwer Academic/Plenum Publishers, 1999

plate-like shapes [5,8,17] and incorporated into a commercial scan system [17,16]. Figure 1 shows a schematic of the immersion pulse-echo testing set-up required to use this method and the resulting ultrasonic waveforms. The mathematical derivation for the method [17] results in ultrasonic velocity being calculated according to:

$$V = c\left(\frac{\Delta t}{2\tau} + 1\right) \tag{3}$$

where c is water velocity, 2τ is the pulse-echo time-of-flight as previously defined, and Δt is the pulse-echo time-of-flight difference between the first echo off the reflector plate front surface with and without the sample present, respectively. Water velocity (c) is determined from known relations between water velocity and temperature [2] or by direct measurement using the time difference of ultrasonic wave travel between two transducer linear positions. This thickness-independent ultrasonic imaging method does not require prior knowledge of sample thickness as shown in equation (3) and if engineered for scanning, the effect of thickness variation is eliminated in the resulting image. Precision and relative accuracy associated with this method are estimated at near 1 percent for plate-like samples having machined surfaces [17]. The thickness-independent methods noted here [5,7–10,16–17,20] require access to both sides of the sample, i.e., there is not a single-sided technique available for scanning that will result in thickness-independence.

EXPERIMENTAL

Basic Procedure

In this investigation, the single transducer reflector plate method shown in figure 1 was scaled-up/engineered for tubular-shaped structures, and the results are presented. The method was used to inspect a polymer matrix composite "proof-of-concept" tubular structure that contained machined patches of various depths and an as-manufactured monolithic silicon nitride tubular structure that might be used in "real world" application. Thickness-independent ultrasonic images for these materials are compared to conventional (apparent) pulse-echo velocity images (the latter being obtained using eq. (2)). The thickness-independent ultrasonic imaging method requires at least two scans to collect the necessary time-of-flight information (entire echoes, or times to echo peaks or edges) (fig. 2). The first of the two scans is run with the sample in place and the time-of-flight information associated with echoes FS (front surface echo), B1 (first back surface echo), B2 (second back surface echo), and M' (first echo off reflector plate front surface with sample present) is collected. Following this, the sample is removed and a second scan is run to collect the time-of-flight information associated with M" (first echo off reflector plate front surface with sample removed). In this investigation, three scans were used to obtain all echo time-of-flight information as required using the version of this method that is commercially-available [16]. FS and B1, or B1 and B2 time-of-flight information were obtained in scan 1, M' time-of-flight information was obtained in scan 2 and M" time-of-flight information was obtained in scan 3. Echo cross-correlation during the first scan, or times to echo peaks and/or edges during any of the scans, were used to obtain time delays 2τ and Δt (eq. (3)). Entire echo digitization and storage was not required in this investigation as it was in [8]. (Obtaining timing information in this manner resulted in slower scan speed but a major reduction in storage required, near-instantaneous velocity image calculation, and more flexibility in capturing desired echo feature times as compared to that for [8]. For best absolute accuracy, it is still recommended that all waveforms be digitized and stored and subsequent time delay calculated using cross-correlation.) As shown in figure 2(a), a tube was placed upon a motorized turntable assembly placed in the immersion

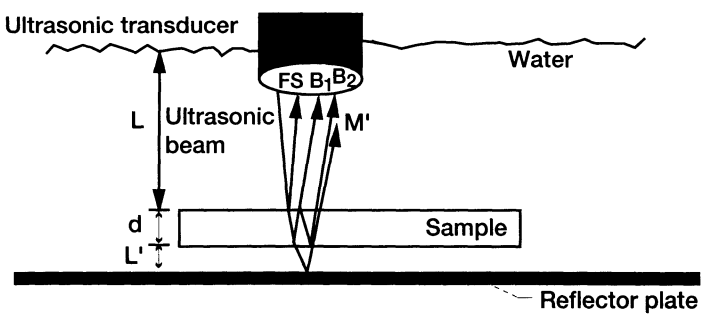

Figure 1.— Single transducer reflector plate method used in this investigation.

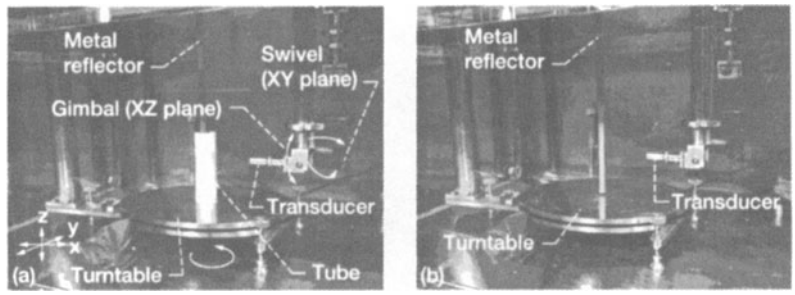

Figure 2.—Ultrasonic scan set-up using turntable scan to obtain thickness-independent velocity images. (a) Scan 1: sample present, collect B1, B2, M'. (b) Scan 2: sample removed, collect M".

scan tank. A machined stainless steel or brass reflector plate was suspended from the scanner bridge and positioned internal to the tube approximately 1 cm from the inside wall. In this manner, the reflector plate remained stationary throughout the scan. Prior to the scan, the transducer was positioned perpendicularly to the tube front surface using lateral, gimbal and swivel adjustments to obtain highest front surface reflection near the scan start position. Then, the distance between the transducer and tube was adjusted starting from the focal length to that distance where tube back surface echoes and reflector echoes were highest. The scanning proceeded as follows. The turntable spun so that one scan line corresponded to a full rotation (360°) of the tube. Ultrasonic data was obtained every 1°. After the turntable completed a full rotation and thus returned to the scan starting position, the transducer was stepped up in height 1 mm so that a new 360° line of data could be obtained. Images were contrast-expanded to better reveal *global* material variation by replacing relatively high and/or low (abnormal) data values that occurred in very low numbers with overall average values that occurred in the original image. Color schemes for the specific images were chosen based on optimum viewing of variations for the examiner but all contained 235 discrete levels.

Material Description and Experimental Parameters

Table I describes the tubular samples and the experimental scan parameters used to obtain the apparent and thickness-independent ultrasonic velocity images for each sample. All transducers were the spherically-focused, longitudinal wave type. Scan and step increment were 1 deg and 1 mm, respectively. The echo features (entire echo, leading edges, peaks) used to obtain differences in time-of-flight (DTOF) 2τ and Δt (eq. (3)) were acquired during the scan and optimized for each sample tube based on the characteristics of the echoes. Analog-to-digital sampling rate was 250 MHz providing a time resolution of 4 ηsec. See [18] for a discussion of timing issues.

TABLE I.—MATERIAL DESCRIPTION AND EXPERIMENTAL PARAMETERS FOR TUBULAR SAMPLES

Tube material and description	Experimental scan parameters	Echo features used for 2τ DTOF calculation method	Echo features used for Δt DTOF calculation method[a]
Polymer Matrix Composite (PMC) "proof-of-concept" sample. Nominal wall thickness 4.1 mm, 152 mm outside diameter, and 176 mm height. Five square 25 × 25 mm patches of depth ~0.1, 0.2, 0.3, 0.5, and 0.8 mm were machined out of the INTERIOR surface of the PMC tube to create thickness variation of up to 20 percent in the tube.	• 2.25 MHz transducer • 360 deg × 60 mm height strip	FS, B1 entire echoes, negative correlation.	Time to M', M" echo absolute peak below 100 percent FSH (video mode).
Silicon Nitride Monolithic Ceramic for high temperature structural application. Nominal wall thickness 7.5 mm, 48 mm outside diameter, and 150 mm height. It was manufactured unintentionally with a 0.8 mm thickness variation (approximately 10 percent of total thickness) and some microstructural variation.	• 20 MHz transducer • 360 deg × 130 mm height strip	B1, B2 entire echoes, positive correlation.	Time to M', M" echo (+)leading edge at (+)100 percent FSH (rf mode).

[a]FSH = Full Scale Height of the on-screen digital oscilloscope.
- video mode = rectified waveform, oscilloscope bounds = 0, 100 percent.
- rf mode = unrectified waveform, oscilloscope bounds = ±100 percent.

RESULTS AND DISCUSSION

Proof-of-Concept Polymer Matrix Composite (PMC) Tube

Consider figure 3 where an unwrapped image of apparent and thickness-independent velocity for a 60 mm height slice of the PMC tube encompassing the machined-in patches are shown. The apparent velocity image of figure 3(a) clearly shows the patches with apparent velocity values increasing as material thickness decreases as expected based on equation (2). (Remember that the value of thickness (d) input for the calculation of the apparent velocity image remains constant while time delay 2τ is decreasing as the material thickness decreases.) Patch edges appear "stepped" due to the coarse scan height increment (1 mm) employed and wave interference (diffractive scattering) present at sharp edges. The thickness-independent velocity images of figure 3(b) shows all five patches have nearly the same velocity except for some remaining indications around the edges. The surrounding material shows minor velocity versus position variation. The results on the "proof of concept" sample indicate the feasibility of using this technique on tubular/curved structures.

Silicon Nitride Tube

Figures 4 and 5 show imaging results for a 130 mm height portion of the silicon nitride tube having a 0.8 mm (10 percent) thickness variation and some microstructural variation. The image results are shown as decaled onto tubular models. A funnel-like feature showing decreasing velocity from tube bottom-to-top is indicated in the apparent velocity image of figure 4(a). This feature disappears in the thickness-independent image of figure 4(b) indicating it was due to thickness variation. Now consider the apparent velocity image of figure 5(a) which was rotated 180° (about the height axis) from the view shown in figure 4(a). For this orientation, an oval-like feature is indicated which is ~14 percent greater apparent velocity than that for the funnel-like region. In the thickness-independent decal image of figure 5(b) (which is the same rotational orientation as that of the apparent velocity image decal shown in fig. 5(a)), the region where the oval existed now shows ~3 percent lower velocity than that for the region where the funnel existed. These results indicate that thickness and microstructural variations are present in the tube. The thickness variations in the two regions of the tube (funnel- and oval-like in apparent velocity image) were confirmed using x-ray computed tomography (CT) slices [18].

Conventional x-ray film radiography and destructive metallographic analysis were used to confirm and determine the nature of the velocity variations seen in the thickness-independent velocity image. Radiography was performed at high and low velocity tube regions (noted on figs. 4(a) and 5(a)) where thicknesses were nearly identical (within 0.8 percent). The film was placed against the inner wall so that the resulting x-rays averaged through the wall thickness. The higher velocity location showed an x-ray

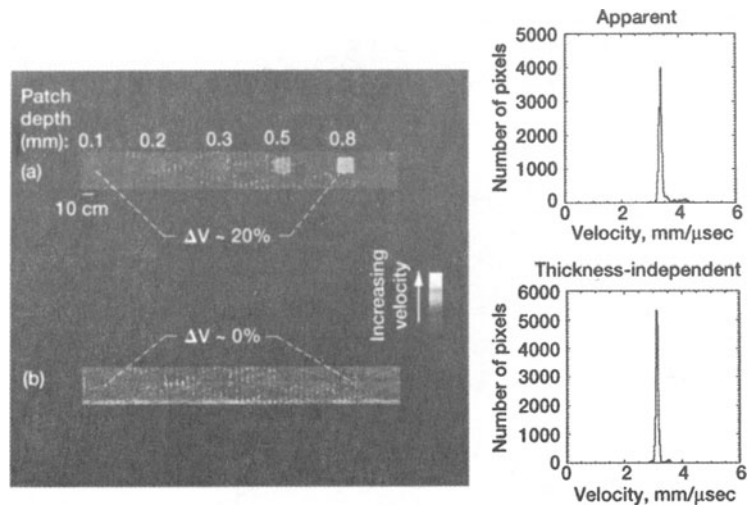

Figure 3.—Apparent and thickness-independent velocity images, and histograms of velocity values for a 60 mm height strip of polymer matrix composite tube containing the machined-in patches. (a) Apparent velocity image. (b) Thickness-independent velocity image.

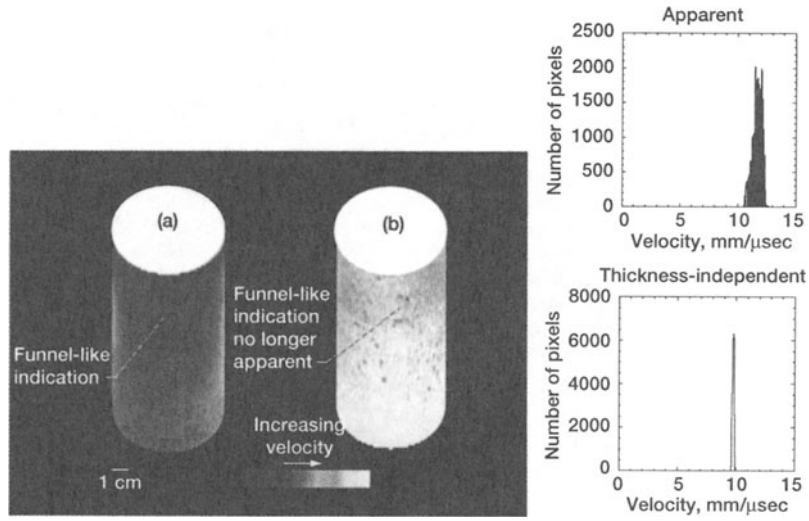

Figure 4.—Apparent and thickness-independent velocity images of silicon nitride tube as decaled onto tubular models. Baseline orientation. (a) Apparent velocity image. (b) Thickness-independent velocity image.

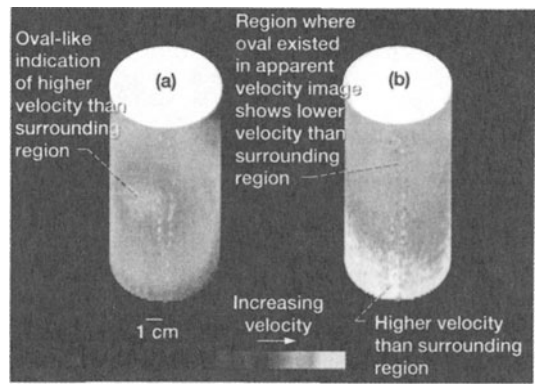

Figure 5.—Apparent and thickness-independent velocity images of silicon nitride tube as decaled onto tubular models. View 180° rotated from baseline orientation. (a) Apparent velocity image. (b) Thickness-independent velocity image.

density of 2.9 while the lower velocity section showed an x-ray density of 3.02, an ~3 percent difference. The higher x-ray density value indicates more x-rays were received at the film which in turn indicates a more porous, less physically-dense material for the lower velocity section. This result is consistent with prior studies showing (1) ultrasonic velocity to be linearly proportional to physical density for silicon nitride [11] and (2) x-ray density to be inversely proportional to physical density for silicon nitride [19]. Metallographic examination of the tube confirmed variable pore fraction throughout the tube. Looking at the cut and polished cross-sectional rings, pore fraction variation was seen to vary (1) within the center area from cross-sectional location to cross-sectional location and (2) from outer to inner edge. (The silicon nitride material is actually a multiphase solid composed of β-silicon nitride grains surrounded by a glass phase between the grains. The glass phase percentage was found to be approximately 18±2% at six locations using backscatter electron microscopy. On the other hand, porosity percentage was found to vary from 0.3 to 2.2±0.1% at the same six locations, a much more significant variation than for the glass phase. Additionally, porosity variation is likely to have a much more significant impact on velocity than would solid phase variation.)

Refraction Effects

In general, tubular structures can be difficult to inspect in the pulse-echo mode in a scan array fashion if the tube is out-of-round at some locations. This is because ultrasound bends, or refracts, when impinging

upon surfaces that are not orthogonal/perpendicular to it. Parallelism between inside and outside surfaces of the tubular structures, and perpendicular incidence of the impinging ultrasonic beam on the sample surfaces and reflector plate, is important to avoid refractive effects that lead to reduced accuracy in the resulting velocity image [4]. Experiments were performed on a tubular structure to investigate the effect of change in ultrasonic beam incidence on echo time-of-flight (TOF), difference in time-of-flight between two echoes (DTOF), Velocities (V) and peak amplitudes (PAs). Gimbal and Swivel angles for the transducer (fig. 3(a)) were changed to simulate surface nonparallelness/out-of-roundness for a mullite ceramic tube of similar dimensions to that of the silicon nitride tube used in this investigation. Detailed results are given in another reference [18] and summarized as follows. The results show that (1) changes tend to be consistent, i.e., $\%\Delta B1 \cong \%\Delta B2$ for TOF and PA changes, (2) TOF, DTOF and V change insignificantly (< 0.5 percent) with changes in gimbal angles less than ~5 deg, (3) TOF, DTOF and Velocity change insignificantly with changes in swivel angles less than ~0.3 deg which was the largest swivel angle change possible; (4) PA generally changes drastically (70 to 100 percent) with changes in gimbal and swivel angles, and (5) small swivel angle (sideways) changes result in significantly more dramatic changes in PA than do small gimbal angle changes. Points (2) and (3) just stated indicate that TOF-based ultrasonic images of tubular samples having some out-of-roundness/nonparallelness of surfaces will contain only small error (if echoes are still measurable, ie. if echoes have not completely disappeared due to misalignment.) Points (4) and (5) just stated lead one to conclude that because of the severe effect that out-of-roundness has on peak amplitude, it is difficult to interpret the results of peak amplitude c-scans where backwall echoes are gated for tubular structures. This effect will be especially severe for small tubes or curved structures having tight radii.) Based on these experiments, it is the opinion of the authors that peak amplitude c-scans of curved structures may not be accurate unless carefully setting up for continuous perpendicular incidence of the ultrasonic beam on the structure surface, and/or parallel structure surfaces are present. At locations in a real tubular sample exhibiting out-of-roundness/ nonparallelness of surfaces such that echoes are reduced to below gate thresholds in a TOF-based scan, it is suggested that an average of nearest neighbors is used at those locations to provide a continuous TOF/DTOF/V image. To summarize, inside and outside surfaces of the tubular structures should be nearly parallel to each other and perpendicular to the impinging ultrasonic beam to avoid refractive effects that lead to reduced accuracy in the resulting velocity image, but some out-of-roundness/nonparallelness of surfaces can be tolerated allowing more practical application. This is a major advantage of the method over peak amplitude-based ultrasonics which are drastically-affected by refractive conditions resulting from out-of-roundness.

CONCLUSIONS

Prior studies described a pulse-echo time-of-flight based ultrasonic imaging method that requires using a single transducer in combination with a reflector plate placed behind samples that eliminates the effect of thickness variation in the image. In those studies, this method was successful at isolating ultrasonic variations due to material microstructure in plate-like samples of silicon nitride, metal matrix composite, and polymer matrix composite. In this study, the method is engineered for inspection of more complex-shaped structures–those having (hollow) tubular/ curved geometry. The experimental inspection technique and results are described as applied to a polymer matrix composite "proof-of-concept" tubular structure that contain machined patches of various depths and an as-manufactured monolithic silicon nitride ceramic tubular structures which might be used in "real world" application. The method proved highly successful at eliminating gross thickness variation effects in the images of the proof-of-concept tubes, and the silicon nitride "real world" tubes. For the silicon nitride tube, conventional film radiography and destructive metallographic analysis confirmed the presence of microstructurally-different regions first revealed by different velocity indications in the thickness-independent ultrasonic image. The microstructual difference was density/pore fraction which agrees with results from prior studies on silicon nitride and other powder metallurgy products. In general, inside and outside surfaces of the tubular structures should be nearly parallel to each other and perpendicular to the impinging ultrasonic beam to avoid refractive effects that lead to reduced accuracy in the resulting velocity image, but some out-of-roundness/nonparallelness of surfaces can be tolerated allowing more practical application. This is a major advantage of the method over peak amplitude-based ultrasonics which are drastically-affected by refractive conditions resulting from out-of-roundness. It is believed that the use of this method can result in significant cost savings because the ultrasonic image, and consequently assessment of tube material and manufacturing quality, can be interpreted correctly in the presence of thickness variations.

REFERENCES

1. Bowles, K., et al., 1992, Void Effects on the Interlaminar Shear Strength of Unidirectional Graphite-Fiber-Reinforced Composites. J. Comp. Mat., Vol. 26, No. 10, pp. 1487–1509.
2. Birks, A.S., et al., eds., Nondestructive Testing Handbook, second edition, Volume 7 Ultrasonic Testing, American Society For Nondestructive Testing, 1991, pp. 225, 227–230 and 237.
3. Christensen, R.M., 1979, Mechanics of Composites, John Wiley & Sons, pp. 47, 51 and 52.

4. Chu, Y.C., et al., 1994, Comparative analysis of through-transmission ultrasonic bulk wave methods for phase velocity measurements in anisotropic materials, J. Acoust. Soc. Am. Vol. 95, No. 6, p. 3205.
5. Dayal, V., 1992, An Automated Simultaneous Measurement of Thickness and Wave Velocity by Ultrasound, Experimental Mechanics, September, Vol. 32, No. 2, pp. 197–202.
6. Flynn, D.R., 1968, Thermal Conductivity of Ceramics, Proceedings of Mechanical and Thermal Properties of Ceramics Symposium, pp. 92–93.
7. Hsu, D.K., et al., 1992, Simultaneous ultrasonic velocity and sample thickness measurement and application in composites. J. Acoust. Soc. Am. Vol. 92, No. 2, Pt. 1, pp. 669–675.
8. Hughes, M.S. et al., 1994, An automated algorithm for simultaneously producing velocity and thickness images, Ultrasonics, Vol. 32, No. 1, pp. 31–37.
9. Kuo, I.Y., et al., 1992, A novel method for the measurement of acoustic speed. J. Acoust. Soc. Am. Vol. 88, No. 4, pp. 1679–1682.
10. Pichè, L., 1994, Ultrasonic velocity measurement for the determination of density in polyethylene. Polymer Engineering and Science, Vol. 24, No. 17, pp. 1354–1358.
11. Roth, D.J., et al., 1991a, "Review, Modeling and Statistical Analysis of Ultrasonic Velocity-Pore Fraction Relations in Polycrystalline Materials," Mater. Eval., Vol. 49, No. 7, pp. 883–888.
12. Roth, D.J. et al., 1991b, "Spatial Variations in a.c. susceptibility and microstructure for the $YBa_2Cu_3O_{7-x}$ superconductor and their correlation with room-temperature ultrasonic measurements, J. Mater. Res. 6[10] pp. 2041–2053.
13. Roth, D.J., et al., 1993, "NDE Approaches for Characterization of Microstructural Variations in Ceramic and Metal Matrix Composites," Proceedings 1993 HITEMP conference, Cleveland, Ohio.
14. Roth, D.J., et al, 1995a, An NDE Approach For Characterizing Quality Problems in Polymer Matrix Composites. Proceedings of the 40th International SAMPE Symposium, 1995, pp. 288–299.
15. Roth, D.J., et. al., 1995, Quantitative Mapping of Pore Fraction Variations in Silicon Nitride Using an Ultrasonic Contact Scan Technique. Res. Nondestr. Eval., Vol. 6, pp. 125–168.
16. Roth, D.J., et. al., 1996, Commercial Implementation of Ultrasonic Velocity Imaging Methods via Cooperative Agreement Between NASA Lewis Research Center and Sonix, Inc. NASA TM–107138.
17. Roth, D.J., 1997, Using a Single Transducer Ultrasonic Imaging Method to Eliminate the Effect of Thickness Variation in the Images of Ceramic and Composite Plates, J. Nondest. Eval., Vol. 16, No. 2.
18. Roth, D.J., et. al., 1998, Scaling up the Single Transducer Thickness-Independent Ultrasonic Imaging Method for Accurate Characterization of Microstructural Gradients in Monolithic and Composite Tubular Structures. NASA TM–1998-206625.
19. Sanders, W.A., et al., 1988, "Correlation of Processing and Sintering Variables with the Strength and Radiography of Silicon Nitride," Advanced Ceramic Materials, Vol. 3, No. 1, pp. 88–94.
20. Sollish, B.D.: Ultrasonic Velocity and thickness gage, United States Patent No. 4,056,970, 1977.